Available online at www.sciencedirect.com
SCIENCE DIRECT®
Polymer 45 (2004) 1659–1664
polymer
www.elsevier.com/locate/polymer

Synthesis, fabrication and characterization of poly[3-3′(vinylcarbazole)] (PVK) Langmuir–Schaefer films

Paolo Bertoncello[a,*], Andrea Notargiacomo[b], Claudio Nicolini[a]

[a]Department of Biophysical, M&O Science and Technologies, (DI.S.T.BI.M.O.), University of Genoa, Corso Europa 30, 16132 Genoa, Italy
[b]Department of Physics, Unità INFM., Roma TRE University, Via della Vasca Navale 84, 00146 Rome, Italy

Received 11 September 2003; received in revised form 4 December 2003; accepted 11 December 2003

Abstract

Poly[3-3′(vinylcarbazole)] (PVK) was synthetized with *N*-vinylcarbazole as monomer by oxidative polymerization with ferric chloride. The resulting polymer was then deposited on various solid supports by using Langmuir–Schaefer (LS) method. The pressure–area isotherm of PVK revealed the possibility of compact monolayer formation at air–water interface. Different layers of PVK were doped with iodine vapours. Both scanning probe microscopy and optical microscopy images indicated a good uniformity of the films. The morphology and the thickness of PVK films were investigated using atomic force microscopy. The voltammetric investigation of I_2 doped PVK showed a distinctive electrochemical behaviour. The photoinduced charge transfer across a donor/acceptor (D/A) hybrid interface provided an effective method to study the photoelectrochemical properties of the composite LS films.
© 2004 Elsevier Ltd. All rights reserved.

Keywords: Poly[3-3′(vinylcarbazole)] (PVK); Langmuir–Schaefer films (LS); Atomic force microscopy (AFM)

1. Introduction

Over the past few years, considerable attention has been devoted to the development of low cost photovoltaic device technologies [1–3]. In this context, organic solar cells have the potential advantage of being cheaper and less energy consuming in fabrication, yet they still lack efficiency [4]. So attempts were performed to study various organic materials, such as phthalocyanines, dyes, conducting polymers (polythiophenes, polycarbazoles, polyphenylenes and poly(phenylene vinylenes and their derivatives) [5–14] and organic–inorganic hybrid structures [15–18]. In order to increase the efficiency, it has been shown that such photoactive device must be based on the photoinduced electron transfer from donor type polymer to acceptor molecules. Consequently, a so-called 'bulk heterojunction' is formed between electron donors and acceptors [19]. One way to improve the properties of this polymer for photovoltaic application is to form a charge transfer complex between poly(*N*-vinylcarbazole) (PVK) and a dopant agent. PVK is an electron donor and the dopant must be an electron acceptor. Out of these studies, photoinduced electron transfer from iodine (I_2) doped conjugated polymers (PVK) provided a new opportunity for making efficient plastic photovoltaic cell [20]. The underlying principle is that singlet excitons, which are created in organic semiconductors by photoexcitation, are likely to dissociate into free charges at the donor–acceptor interface [21]. However, in present ~3% power conversion efficiency still hinders it to have commercial success. Further optimization of device performance is currently being carried out. The physical properties of such composite material in organized molecular assemblies will become a focus of interest because of their optical and photovoltaic properties [22,23]. Langmuir–Blodgett (LB), Langmuir–Schaefer (LS) or layer-by-layer techniques have been proven to be powerful tools for the fabrication of ultra-thin polymeric thin films with controlled structures [14,24,25]. Organized LB/LS assemblies are particularly attractive as they allow a very high control of the layer thickness, and require a very small amount of polymer material in contrast to the solution casting or spin coating techniques [26], respectively.

* Corresponding author. Address: Department of Chemistry and Biochemistry, The University of Texas at Austin, 1 University Station, MailStop A5300, Austin, TX 78712, USA. Tel.: +1-5124713249; fax: +1-5124719495.
E-mail address: pbertonc@cm.utexas.edu (P. Bertoncello).

0032-3861/$ - see front matter © 2004 Elsevier Ltd. All rights reserved.
doi:10.1016/j.polymer.2003.12.032

Keeping in view the above properties, Langmuir monolayers of PVK were obtained at air–water interface. Langmuir–Schaefer films were fabricated on various solid supports, and their optical, electrical and electrochemical properties were investigated. The photoelectrochemical properties of iodine doped PVK LS films were also studied.

2. Experimental details

2.1. Synthesis of poly[3-3′(vinylcarbazole)]

N-vinylcarbazole as monomer, ferric chloride ($FeCl_3$) as oxidant agent and various reagents were obtained from Sigma-Aldrich for the synthesis of poly[3-3′(vinylcarba-(vinylcarbazole)] (PVK). The use of $FeCl_3$ as oxidant is necessary to polymerize the monomer at the position of 3, 3′ instead of the vinylic group [27] (see Scheme 1). For instance, 2.5×10^{-3} mol dm^{-3} of $FeCl_3$ were dissolved in chloroform and then filtered using a paper filter. Then, in the ferric chloride solution, 0.1 mol dm^{-3} of tetrabuthylammoniumtetrafluoborate (TBATFB) were added. The addition of the salt as a spacer is a necessary step to have a polymer with short macromolecular chain and to increase the solubility in the most common organic solvents. Separately, 0.1 mol dm^{-3} of monomer (*N*-vinylcarbazole) was dissolved in chloroform. Both solutions were placed in an ice bath in order to maintain a temperature in the range 0–4 °C. The monomer solution was added slowly into the $FeCl_3$ solution containing TBATFB. The reaction was continued for at least 12 h. A dark blue solution was obtained. Then, methanol was added into the mixture at room temperature and the PVK polymer precipitated. The grey polymer obtained was filtered and washed in deionized water several times and after in diethyl ether in order to remove oligomers. The resulting PVK obtained was partially soluble in chloroform.

2.2. Fabrication of Langmuir–Schaefer films of PVK

A homogeneous solution of PVK polymer was obtained in chloroform at 2 mg 5 mL^{-1} by sonicating for 2 h. The resulting solution was filtered using 0.5 μm filter paper. PVK Langmuir monolayer was formed by using Langmuir trough (MDT Co., Moscow, Russia, 240 mm × 100 mm in size and 300 mL in volume). PVK LS films were formed in a subphase containing deionized water (Milli-Q water with a resistivity of 18.2 MΩ cm). After the complete evaporation of spreading solvent (chloroform), the floating film was compressed to record the surface pressure–area isotherms, as well as to deposit the films. The fabrication of PVK LS films was carried out at a surface pressure of 25 mN m^{-1} in all cases with a barrier speed of 1.67 mm s^{-1}. Different layers of PVK were deposited on various solid substrates (quartz, glass, indium tin oxide (ITO) and silicon). Finally, PVK LS films were doped by placing the samples in a chamber containing iodine vapours for at least 24 h. I_2 doped PVK was green indicating the successful doping of the polymer.

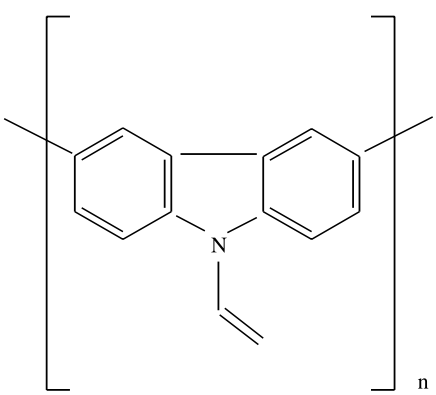

Scheme 1. Schematic of poly[3-3′(vinylcarbazole)] (PVK).

2.3. Atomic force microscopy (AFM) measurements

Atomic force topographies were carried out by using a Digital Instruments D3100 atomic force microscopy (AFM) with Nanoscope IIIa controller operating in air at constant relative humidity of about 60% The AFM worked in 'Tapping Mode' configuration using commercial n^+-doped silicon micro-levers with an apex curvature radius of the probe tip in the 5–10 nm range, and a typical force constant of about 40 N m^{-1}. AFM technique was also used for the estimation of the films thickness by using the following procedure. At first, the film was repeatedly scratched using a cantilever of the same type used for imaging but operating in 'Contact Mode'. The typical value of the force applied for a complete removal of the deposited material was in the 2–5 μN range. These values have been chosen in order to 'open' a clean area of the substrate avoiding its damage. A new probe was then used to scan the scratched area. The film thickness was calculated by averaging several profiles across the scratched area and measuring the vertical distance between the substrate and the film surface. The material pile-up due to scratching is usually only present in an area few hundreds of nanometers wide along the border of the scratch which is not considered for the thickness estimation.

2.4. Optical measurements

Absorption spectra of PVK LS films were recorded using a Jasco spectrophotometer (model V-530). The vibrational bands of PVK on KBr pellets were determined using FTIR spectrophotometer (Bruker V-22) with nominal resolution of 4 cm^{-1} in transmission mode. The sample chamber was continuously purged with nitrogen gas for 20 min before data collection, and during the measurements to eliminate water vapor adsorption. FTIR spectra of PVK were obtained after proper subtraction with recorded silicon baseline.

2.5. Electrochemical and photochemical measurements

The electrochemical measurements were performed using a Potentiostat/Galvanostat EG&G PARC, model 263A controlled by M270 software In all cases, a standard three electrodes cell configuration was used. The working electrode was an indium tin oxide (ITO) coated glass plate on which PVK films were deposited. A platinum coil was used as the counter electrode and Ag/AgCl (KCl saturated) as the reference electrode. The electrochemical experiments were performed using a relative working electrode area (0.3 cm^2) in the solution that was employed to investigate the electrochemical behaviours of PVK LS films. The photoelectrochemical current was measured using a standard cell containing three electrodes. A white light of 150 W was illuminated keeping a distance of 5–10 cm from the working electrode for the photoelectrochemical current response.

3. Results and discussion

3.1. Langmuir isotherm

Fig. 1 shows the surface pressure–area (Π–A) isotherm of Langmuir monolayer of PVK as a function of barrier speed. The isotherms reveal a condensed shape. In general, the stability of Langmuir film is usually associated with a high collapse pressure, a steep increase in the condensed phase and a small hysteresis in a compression–expansion cycle [28,29]. As can be seen in Fig. 1, the isotherm reveals a high collapse pressure (smooth collapse begins at about 60 mN m^{-1}) and a steep increase in the condensed phase. Due to difficulties in determining the real molecular weight and the exact solubility of the available PVK, the isotherms report the barrier distance as the unit on the X-axis. The barrier's speed does not seem to influence the isotherm behaviour as evidenced in Fig. 1 (curves a–c). Based on the isotherm investigations, we have deposited LS films of PVK at a surface pressure of 25 mN m^{-1} and at a barrier speed of 1.67 mm s^{-1}.

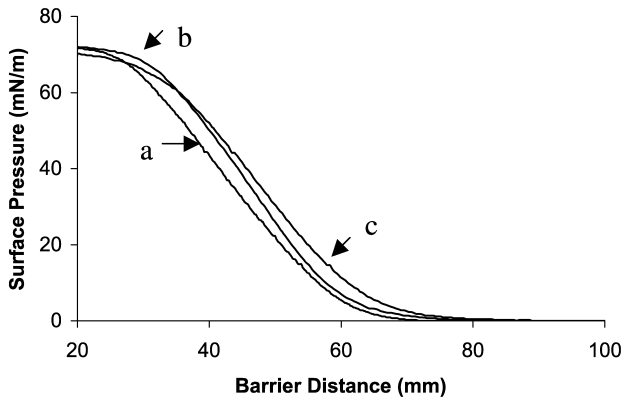

Fig. 1. Π–A isotherms of PVK as a function of barrier speed: (a) 1.67 mm s^{-1}, (b) 1 mm s^{-1}, (c) 0.5 mm s^{-1}.

3.2. AFM measurements

The morphology of PVK films investigated using AFM Fig. 2 shows the 6 μm × 6 μm topographies of undoped (a) and doped (b) 5 layers PVK LS film samples deposited on silicon substrate. The substrate surface is entirely covered by the films. The undoped sample shown in Fig. 2(a) has a uniform topography with some few nanometers thick clusters. A more accurate investigation on a 0.7 μm × 0.7 μm area reveals the presence of grains with diameter down to about 40 nm. The doped sample shown in Fig. 2(b) shows several hundreds of nanometers thick structures distributed on a regular grain-like surface. In the 0.7 μm × 0.7 μm scan the grains, about 50–100 nm wide, appear to be arranged in clusters. The film thickness is obtained following the procedure described in Section 2.4. For the five layers sample, shown in Fig. 3, the average thickness, measured on areas free of clusters, is found to be ~28 nm, providing an estimation of 5.6 nm per layer. Of course, such a value of thickness cannot correspond to the cross-section of the polymer chain. However, the polymer can form branched layers at the air/water interface during compression, which can be then transferred onto solid substrates. Therefore, the thickness of the layer transferred during one dipping can be much more than the chain cross-section.

3.3. UV–Vis and FTIR measurements

A typical spectrum of PVK LS films is shown in Fig. 4. This spectrum corresponding to 15 layers deposited on quartz substrate depicts an absorption threshold at about 350 nm and absorption peaks at 340, 290, 260, 240 nm. The effect of iodine doping is clearly evidenced in Fig. 4 (curve b and c) with the appearance of a new wide peak at about 380 nm. These results are in agreement with UV–Vis spectra of I_2 doped PVK reported in literature [30,31].

The spectrum of PVK powder obtained in KBr pellet (figure not shown) is consistent with the infrared spectrum of PVK reported in literature [32] and evidences the

Table 1
FTIR peak assignment of (PVK)

Wavenumber (cm^{-1})	Peak assignments
2950	Aromatic C–H asymmetric stretching
1630–1600	C=C stretching of vinyledine group
1480–1460	Ring vibration of *N*-vinylcarbazole moiety
1410	$>CH_2$ deformation of vinyledine group
1330	C–H deformation of vinyledine group
1230–1220	C–N stretching of vinylcarbazole
1160–1130	C–H in plane deformation of aromatic ring
723	Ring deformation of substituted aromatic structure

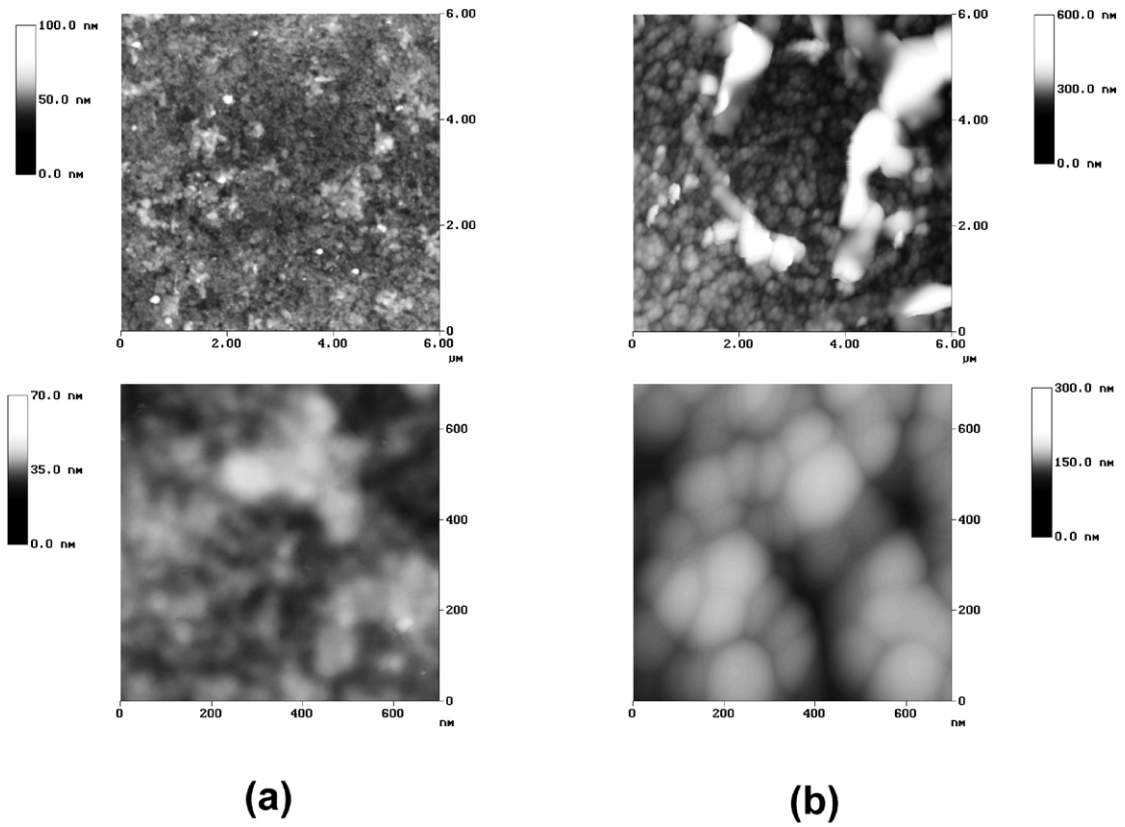

Fig. 2. AFM topographies of 5 layers PVK LS films (a) and five layers I_2 doped PVK LS films (b). For each sample two scan sizes are reported: 6 and 0.7 μm, respectively. The bar aside each scan shows the height vs. greyscale correspondence. Note that different height scales are used to optimize the view of surface features.

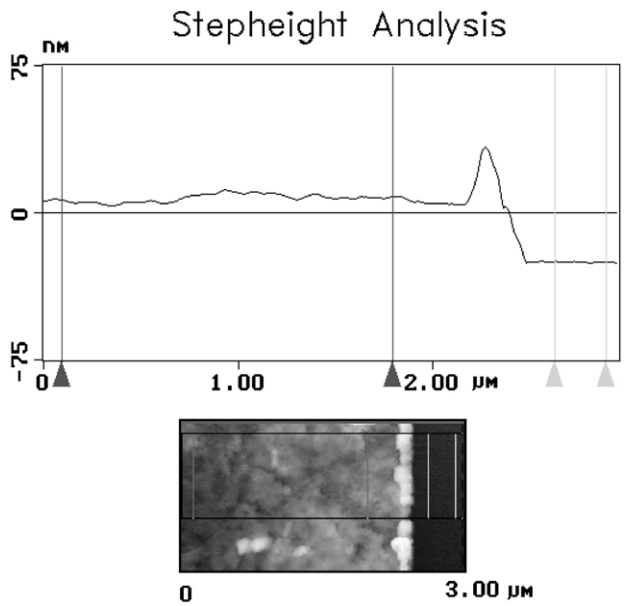

Fig. 3. Typical profile of a PVK film after scratching an area with AFM tip. A thickness of ~28 nm is found for the five-layer film reported in figure by measuring the average vertical distance between the two couples of markers. The 3 μm × 1.5 μm plan-view located below the profile shows the area considered for the step-height analysis. The film and substrate surface is depicted in light and dark grey, respectively.

formation of the PVK moiety. Detailed band assignments of PVK powder are presented in Table 1.

3.4. Electrochemical measurements

Fig. 5 shows the cyclic voltammogram of I_2 doped 30 layers PVK LS films registered in 10^{-2} mol dm^{-3} $LiClO_4$, scan rate 20 mV s^{-1}. It reveals only one broad reduction peak at −190 mV (vs. Ag/AgCl). This peak is attributed to the reduction of the complex formed between I_2 and PVK LS films. The peak cannot to be attributed to the reduction of iodine: in fact, as reported in literature, the reduction of

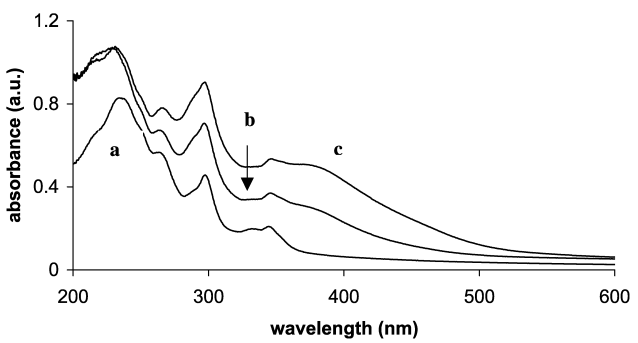

Fig. 4. UV–Vis spectra of 15 layers PVK LS films (a), 15 layers PVK LS films after doping in I_2 vapours for 30 min, 15 layers PVK LS films after doping in I_2 vapours for 60 min.

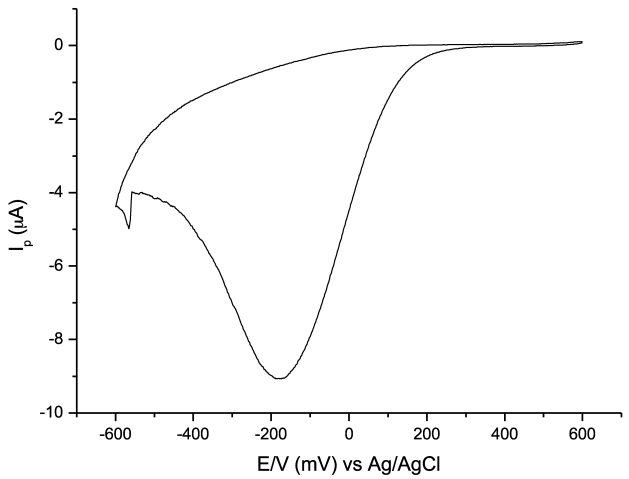

Fig. 5. CV of I_2 doped 30 PVK LS films scanned from 0.6 to −0.6 V, supporting electrolyte: 10^{-2} mol dm^{-3} $LiClO_4$, scan rate 20 mV s^{-1}.

iodine occurs at about 0.3 V (vs. SCE) and its oxidation at higher positive potential [33,34]. Interestingly, no peaks were observed if the doping process time is short (<24 h.), indicating a slow kinetics of the process. When the system is cycled at a potential lower than −0.6 V, the peak disappears completely. In this case, we observed that the colour of the film changes from green to pale blue, indicating a complete dedoping of the sample. Based on this observation, we have performed the photocurrent measurements in the range from 0.5 to −0.1 V in order to avoid the complete dedoping of the films.

Fig. 6 shows the linear sweep voltammetry (LSV) of 30 layers of I_2 doped PVK registered without illumination (a) and under illumination (b). The LSV under illumination conditions shows a similar feature to that of 30 layers without illumination. It reveals an increase in the current of about 600 nA cm^{-2} in the voltage range from 0.1 to 0.3 V when the films are under illumination. For the generation of electrical power by illumination it is necessary to separate spatially the electron–hole (e–h) pair generated during the absorption process before a recombination takes place. In conjugated polymers, the effective separation of the photoexcited e–h pair can be achieved by blending the polymer with an acceptor molecule having an electron affinity which falls the inequality ($I_p^* - E_a - U_{eff} < 0$), where I_p^* is the ionization potential of the excited donor, E_a, the electron affinity of the acceptor and U_{eff}, all Coulomb correlations including the polarization effects. Under these conditions, it is energetically favourable for the excited conjugated polymer to transfer an electron to the acceptor molecule, while a hole remains in the polymer valence band.

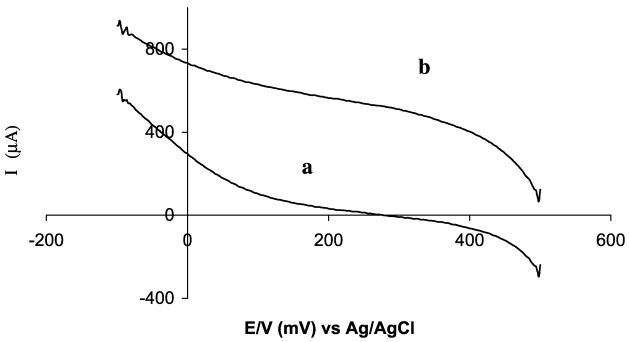

Fig. 6. LSV of I_2 doped 30 layers PVK LS films scanned from 0.5 to −0.1 V: (a) without illumination; (b) under illumination; supporting electrolyte: 10^{-2} mol dm^{-3} $LiClO_4$; scan rate: 20 mV s^{-1}.

3.5. Photocurrent measurements

For photocurrent measurements, a 150 W white lamp used as a source of whole wavelength was passed through ITO/I_2 doped PVK LS films employed as photoanode in a photoelectrochemical cell. A steady electrochemical photocurrent was observed applying potential by potentiostat. The photocurrent generation was prompted and responded to on/off cycles of illumination. Fig. 7 shows the photocurrent transient for I_2 doped 30 layers PVK LS films. The potential of the working electrode was set at 0.4 V (vs. Ag/AgCl). A fast and uniform photocurrent response was observed in each switch-on and switch-off condition, which is related to ion transport in the electrolyte, but is more dependent on the p–n interface in the nanocomposite films. Such a figure shows that the photocurrent rise time is shorter than the time between light switch-off and switch-on for PVK LS films. The increase in the current of the sample under illumination is about 300 nA cm^{-2} and is strictly dependent on the applied potential. The higher photocurrent is observed at 0.4 V and it decreases when the applied potential is shifted to negative values. As the applied potential is scanned towards the positive potentials, we observed an increase in the photocurrent generation. Increased charge separation and the facile transport of charge carriers under positive bias resulted in the enhanced photocurrent generation. The decrease in the current at lower applied potentials is in agreement with the voltammetric data that indicate an irreversible reduction with concomitant dedoping of the films. This fact suggests that the device efficiency can be enhanced with the increase in the doping level of I_2 in the PVK LS films. Through these studies, an effective

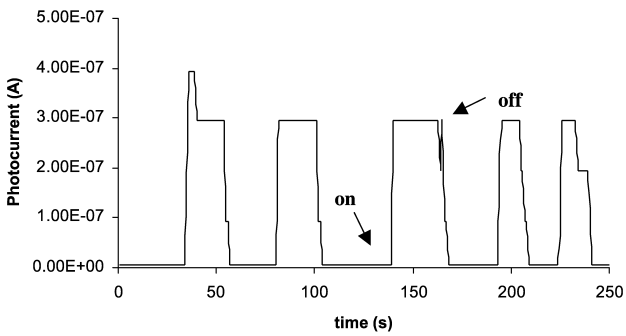

Fig. 7. The photoelectrochemical current for I_2 doped 30 layers PVK LS films at 0.4 V in 10^{-2} mol dm^{-3} $LiClO_4$: (a) switch-on; (b) switch-off.

composite can be carefully selected and the solid photovoltaic devices will be investigated further.

Further investigations are in progress to increase the stability and the photocurrent performances of PVK LS films utilizing LiI and I_2 as supporting electrolyte and dopant, respectively.

4. Conclusions

We have synthetized PVK by oxidative polymerization with ferric chloride of *N*-vynilcarbazole. FTIR spectrum revealed the formation of the polymer. The Π–A isotherm of PVK revealed the possibility of formation of compact monolayer at the air–water interface.

AFM investigation confirmed the complete surface coverage and have shown the presence of grains, larger in sizes and arranged in clusters in the doped sample. UV–Vis measurements evidenced the typical peaks of PVK and the effect of iodine doping. By the aid of electrochemical methods, we can tune up the nanocomposite material to get the maximum photocarrier generation efficiency. Under illumination, the increase in photocurrent is about 300 nA cm^{-2}. The photoinduced charge transfer across a donor/acceptor (D/A) hybrid interface provided an effective method to study the photovoltaic properties of composite LS films.

Acknowledgements

We are grateful to Dr V. Erokhin (I.N.F.M.—University of Parma) and Dr M.K. Nam (Fractal Systems Co., USA) for useful discussion and Dr V. Bavastrello (University of Genoa) for his help during the synthesis of PVK polymer. Financial supports from F.I.R.B., 'Organic Nanoscale Science and Technology'.

References

[1] Roman LS, Andersson MR, Johannes T, Inganas O. Adv Mater 1997; 9:1164.
[2] Halls JJM, Walsh CA, Greenham NC, Marseglia EA, Friend RH, Moratti SC, Holmes B. Nature 1995;376:498.
[3] Yu G, Gao J, Hummelen JC, Wudl F, Heeger J. Science 1995;270: 1789.
[4] (a) Roman LS, Mammo L, Pettersson AA, Andersson MR, Inganas O. Adv Mater 1998;10:774. (b) Yu G, Heeger AJ. J Appl Phys 1995;78: 4510. (c) Yu G, Heeger AJ. Synth Met 1997;85:1183.
[5] (a) Brabec CJ, Padinger F, Hummelen JC, Janssen RAJ, Sariciftci NS. Synth Met 1999;102:861. (b) Bernede JC, Alimi K, Safoula G. Polym Degrad Stab 1999;46:269.
[6] Padinger F, Brabec CJ, Fromherz T, Hummelen JC, Sariciftci NS. Opt Rev 2000;8:280.
[7] Hagen J, Li Y, Haarer D. Synth Met 1998;94:273.
[8] Padmanaban G, Ramakrishnan S. J Am Chem Soc 2000;122:2244.
[9] Marumoto K, Takeuchi N, Ozaki T, Kuroda S. Synth Met 2002;129: 239.
[10] Friend RH, Denton GJ, Halls JJM, Harrison NT, Köhler A, Tessler N, Holmes AB, Lux A, Moratti SC, Pichler K. Solid State Commun. 1997;102:249.
[11] Yu G, Zhang C, Pakbaz K, Heeger AJ. Synth Met 1995;71:2241.
[12] Wei X, Frolov SV, Vardeny ZV. Synth Met 1996;78:295.
[13] Ram MK, Sarkar N, Bertoncello P, Sarkara A, Narizzano R, Nicolini C. Synth Met 2001;122:369.
[14] (a) Ding H, Bertoncello P, Ram MK, Nicolini C. Electrochem Commun 2002;4:503. (b) Ram MK, Carrara S, Paddeu S, Nicolini C. Langmuir 1997;13:2760. (c) Bertoncello P, Notargiacomo A, Ram MK, Riley DJ, Nicolini C. Electrochem Commun 2003;5:787.
[15] Graham SC. Synth Met 1997;84:903.
[16] Seki K, Tani T, Ishii H. Thin Solid Films 1996;273:20.
[17] Kim H, Kim JY, Lee K, Park Y, Jin Y, Suh H. Curr Appl Phys 2001;1: 139.
[18] Yu G, Gao J, Hummelen JC, Wudl F, Heeger AJ. Science 1995;270: 1789.
[19] Brabec CJ, Sariciftci NS. Mater Today 2000;3:5.
[20] Safoula G, Touihri S, Bernede JC, Jamali M, Rabiller C, Molinie P, Napo K. Polymer 1999;40:531.
[21] (a) Xiao Y, Yu WL, Pei J, Chen Z, Huang W, Heeger AJ. Synth Met 1999;106:165. (b) Konarev DV, Drichko NV, Lyubovskaya RN, Shulga YuM, Litvinov AL, Semkin VN, Dubsitsky YuA, Zaopo A. J Mol Struct 2000;526:25.
[22] Dyakonov V. Physica E 2002;14:53.
[23] Liess M, Lane PA, Kafafi ZH, Vardeny ZV. Synth Met 1997;84:683.
[24] Ram MK, Bertoncello P, Nicolini C. Electroanalysis 2001;13:574.
[25] Ram MK, Adami M, Faraci P, Nicolini C. Polymer 2000;41:7499.
[26] Ghayoury AE, Schenning APHJ, Hal PAV, Weidl CH, Dongen JLJV, Janssen RAJ, Schubert US, Meijer EW. Thin Solid Films 2002;403:9.
[27] Siove A, David A, Ades D, Roux C, Leclerc M. J Chim Phys 1995;92: 787.
[28] Ulman A. An introduction to ultrathin organic films: from Langmuir–Blodgett to self-assembly. Boston, MA, USA: Academic Press; 1991.
[29] Petty MC. Langmuir–Blodgett films: an introduction. Cambridge, UK: Cambridge University Press; 1996.
[30] Ouro Djobo S, Bernede JC, Napo K, Guellil Y. Mater Chem Phys 2002;9405:1.
[31] Pfister G, Griffits EH. Phys Rev Lett 1978;40:659.
[32] He R, Qian X, Yin J, Bian L, Xi H, Zhu Z. Mater Lett 2003;57:1351.
[33] Walcarius A, Lefevre G, Rapin J-P, Renandin G, Francois M. Electroanalysis 2001;13:313.
[34] Zhang W, Zha H, Yao B, Zhang C, Zhou X, Zhong S. Talanta 1998; 46:711.